JOURNAL OF SOLID STATE CHEMISTRY 54, 330–341 (1984)

Ionic and Metallic Clusters of the Alkali Metals in Zeolite Y*

M. R. HARRISON, P. P. EDWARDS,† J. KLINOWSKI, AND J. M. THOMAS

University Chemical Laboratory, Cambridge University, Lensfield Road, Cambridge CB2 1EW, United Kingdom

AND D. C. JOHNSON AND C. J. PAGE

Baker Laboratory of Chemistry, Cornell University, Ithaca, New York 14853

Received February 15, 1984

Dehydrated samples of zeolite Y containing alkali-metal cations have been reacted with alkali-metal vapor in sealed silica tubes, and the products studied by electron-spin resonance (ESR) spectroscopy. Two distinct species were detected following the reaction of sodium-exchanged zeolite Y with sodium, potassium, or rubidium vapor. Exposure to a low concentration of metal vapor resulted in brightly colored samples with ESR signals characteristic of a stable ionic cluster species Na_4^{3+}, in which an unpaired electron is trapped on four equivalent sodium cations in the sodalite cages of the zeolite. Exposure to higher concentrations of metal vapor resulted in dark-colored samples with ESR signals characteristic of small metallic particles located inside the zeolite cavities. A similar ionic cluster species K_4^{3+} was detected following the reaction of potassium-exchanged zeolite Y with sodium or potassium vapor although the potassium cluster was less stable than its sodium counterpart and an ESR signal from small metallic particles was observed at the same time. The corresponding Rb_4^{3+} ionic cluster species was not detected following the reaction of rubidium-exchanged zeolite Y with rubidium vapor; only an ESR signal from small metallic particles was observed. The narrow linewidths of the ESR signals from the small metallic particles suggest an inhibition of the spin-relaxation mechanisms in the bulk metals.

Introduction

Zeolites are of interest because of their exceptional catalytic properties, attributed in part to the presence of intracrystalline cavities and channels (*1*). The chemical formula of a zeolite containing alkali-metal cations M^+ is $M_x[(AlO_2)_x(SiO_2)_y] \cdot zH_2O$, and the structure is composed of corner-sharing SiO_4 and AlO_4 tetrahedra with exchangeable cations which balance the negative charge of the aluminosilicate framework located within the cavities. The silicon-to-aluminum ratio is therefore an important parameter since it determines the number of exchangeable cations. The water molecules which normally occupy the cavities can be removed by heating, and a variety of organic and inorganic molecules can be absorbed provided their dimensions are comparable with those of the channels.

There are many distinct zeolitic struc-

* Dedicated to Dr. M. J. Sienko.

† Author to whom correspondence should be addressed.

0022-4596/84 $3.00

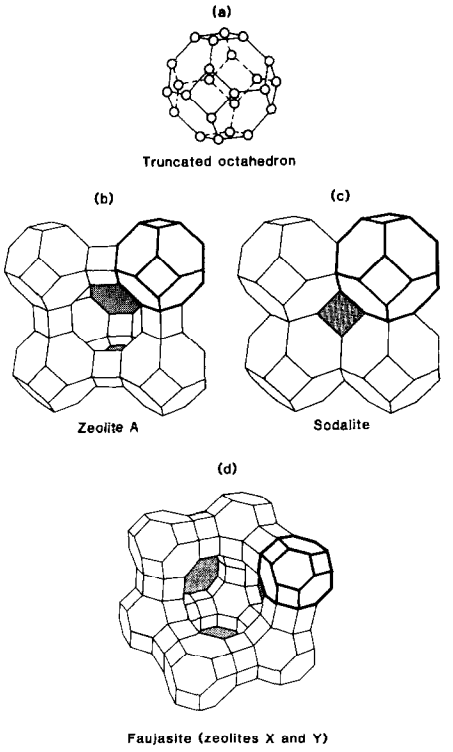

FIG. 1. The sodalite cage and the structure of zeolites belonging to the faujasite family. The vertices of the polyhedra are occupied by the framework silicon or aluminum atoms; the framework oxygen atoms and exchangeable cations are not shown.

tures (*2*), but in this paper we concentrate upon faujasitic zeolites in their sodium, potassium, and rubidium cation-exchanged forms. An outline of the structure of faujasitic zeolites is given in Fig. 1. The vertices of the polyhedra are occupied by the framework silicon or aluminum atoms which are in turn tetrahedrally bonded to the framework oxygen atoms; these oxygen atoms and the exchangeable cations are not shown for clarity. The polyhedron with 14 vertices (tetrakaidecahedron) in Fig. 1a is known as the sodalite or β-cage and is the principal building block of the three structures shown in the figure.

In the mineral sodalite shown in Fig. 1c the neighboring sodalite cages share some silicon and aluminum atoms. The Si : Al ratio of Na-sodalite is always unity, and the silicon and aluminum atoms alternate throughout the framework. Only one type of cavity occurs in sodalite, with a diameter of 6.5 Å and accessed through small six-membered pores 2.2 Å in diameter. There are six alkali-metal cations in each sodalite cage.

Zeolite A (Fig. 1b) is a synthetic mineral with no natural counterpart. The sodalite cages are here connected by double four-membered rings, forming an interconnected set of larger cavities within the material known as α-cages with a diameter of 11.5 Å and accessed through eight-membered pores 4.2 Å in diameter. The Si : Al ratio in zeolite A is generally close to unity and, as in sodalite, the silicon and aluminum atoms alternate throughout the framework. There is one α-cage for every sodalite cage and 12 alkali-metal cations are distributed between them.

Zeolites X and Y (Fig. 1d) are the synthetic counterparts of the naturally occurring mineral faujasite. The sodalite cages are connected by double six-membered rings, forming an interconnected set of even larger cavities within the material also known as α-cages (or supercages) with a diameter of 12.5 Å and accessed through 12-membered pores 7.5 Å in diameter. Zeolites X and Y have the same framework structure, but different Si : Al ratios that can also vary over a considerable range. By convention, the zeolite is labeled X if $1 \leq \mathrm{Si} : \mathrm{Al} < 1.5$ and Y if $1.5 \leq \mathrm{Si} : \mathrm{Al} < 3$. Thus zeolite Y has a smaller concentration of framework aluminum atoms and hence exchangeable cations within the cavities than zeolite X. Since the Si : Al ratio is variable, there are a large number of arrangements possible for the framework silicon and aluminum atoms; the precise arrangement for any particular Si : Al ratio is still a matter of debate although greatly clarified by recent studies (*3*). In the present work we have

used zeolite Y with Si : Al = 2.0. For this composition, there is one supercage for every sodalite cage and eight alkali-metal cations are distributed between them.

Despite the pioneering work of Rabo and Kasai (*4–6*), it is not widely appreciated that unusual polynuclear cationic species, e.g., Na_4^{3+}, can be installed into the zeolite cavities by the use of a reducing agent such as alkali-metal vapor. In this paper, we further investigate the preparation and electronic properties of these compounds using electron-spin resonance (ESR) spectroscopy.

Experimental Methods

Sample Preparation

The Si : Al ratio of the parent zeolite Y containing sodium cations (Na-Y)[1] was determined to be 2.0 by energy-dispersive X-ray analysis in an electron microscope and by magic-angle-spinning ^{29}Si NMR spectroscopy (*7, 8*). Samples exchanged with potassium or rubidium cations were then prepared from the sodium form using standard techniques (*9*).

The samples were exposed to alkali-metal vapor in silica reaction vessels which could be heated inside a tube furnace. An access tube extending outside the tube furnace was attached to one end of the central chamber to enable the reaction vessel to be connected to a vacuum line. An ESR tube was attached to the other end of the chamber to permit the ESR spectrum of the transferred sample to be recorded without exposing the sample to the atmosphere. These ESR tubes were made of Spectrosil silica with a low concentration of paramagnetic impurities.

A suitable amount of the zeolite (typically 1 g) was placed in the central chamber with the access arm open to the atmosphere. The temperature was slowly increased to 400°C and then kept constant for approximately 2 hr to remove the bulk of the zeolitic water. At this stage, the access arm was connected to a vacuum line and the reaction vessel evacuated to below 10^{-4} Torr. The zeolite was finally heated overnight under vacuum to remove the remainder of the water.

The required amount of alkali metal was then added to the zeolite. The metal had previously been purified by melting under vacuum, and forcing it into calibrated capillary tubes. Any oxidation of the alkali metal in the atmosphere was therefore confined to the open ends of the capillary tube, and these were removed immediately before use. The vacuum line was disconnected, and a suitable length of the capillary tube containing the metal placed in the access arm. During this procedure, the zeolite was maintained at 400°C to prevent the reabsorption of water into the zeolite cavities. The vacuum line was reconnected and the reaction vessel reevacuated to below 10^{-4} Torr. The zeolite was then heated under vacuum for approximately 2 hr.

At this stage, the tube furnace was turned off and the zeolite allowed to cool under vacuum. The capillary tube containing the metal was then tipped from the access arm into one end of the central chamber away from the zeolite, and the access arm sealed under vacuum. The metal was extruded from the capillary tube by gently warming the capillary tube with a gas torch. A thin metallic mirror was formed on the inside of the central chamber, and in this form the alkali metal reacted rapidly with the zeolite when the reaction vessel was heated in the tube furnace.

Spontaneous coloration of the zeolite occurred for the sodium samples at ~350°C, for potassium samples at ~250°C, and for rubidium samples at ~150°C. However, it was advantageous to perform the reaction at a lower temperature for a longer time

[1] Zeolite Na-Y was kindly provided by Dr. A. Comyns of the Laporte Company, Widnes, England.

since a degradation of the colored product was observed if the reaction was prolonged. It is possible that the alkali metal starts to attack the aluminosilicate framework, and we are currently investigating this by X-ray diffraction measurements. The degradation is possibly assisted by the presence of residual water in the zeolite cavities since the stability of the product appeared to increase when a more stringent dehydration procedure was adopted.

ESR Measurements

ESR spectra of the powdered samples sealed in the Spectrosil silica tubes were recorded on a Varian E-109 spectrometer at X-band frequencies (9.3 GHz) using a 100-kHz modulation frequency. The temperature of the samples could be continuously varied between 10 and 120 K using helium gas, and between 120 K and room temperature using nitrogen gas. The temperature was measured with a thermocouple positioned in the gas flow path just below the samples, and could be controlled to within 2 K by means of an Oxford Instruments regulator. The g-values could be calculated to within 0.0005 using an internal DPPH standard (g = 2.0036).

We have routinely recorded both the first-derivative and second-derivative ESR spectra of the samples, and these are shown on the left and right, respectively, of Figs. 2, 4, and 5. The increased resolution of the second-derivative ESR spectra was invaluable in the detection of weak or partially resolved hyperfine structure.

Results

Zeolite Y Containing Sodium Cations

The ESR spectra obtained at 120 K from three samples of zeolite Na-Y reacted with sodium vapor are shown in Fig. 2. The concentration of sodium increases from the top to the bottom of the figure, and is given below as the number of sodium atoms per sodalite cage. However, we are unable to determine whether the sodium atoms are dispersed uniformly throughout the zeolite cavities, and it is possible that some of the metal is concentrated near the surface of the crystallites.

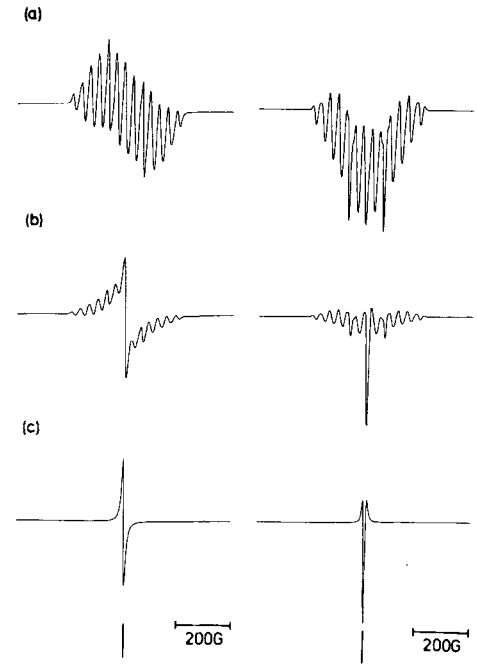

FIG. 2. First-derivative (on the left) and second-derivative (on the right) ESR spectra (120 K) of samples of zeolite Na-Y reacted with sodium vapor. The marker corresponds to a DPPH signal at g = 2.0036. The metal concentration increases from top to bottom.

The most dilute sample is pink, and the amount of sodium metal reacted with the zeolite is equivalent to one additional sodium atom per sodalite cage. On exposure to the atmosphere, the pink color instantly disappeared suggesting that oxygen molecules could rapidly diffuse into the center of the crystallites. The intermediate sample is dark red, and the amount of metal is equivalent to three additional atoms per sodalite cage. The concentrated sample is black, and the amount of metal is equivalent to six additional sodium atoms per sodalite cage.

On exposure to the atmosphere, the black color disappeared slowly over a period of several hours suggesting that rate of diffusion of oxygen molecules into the crystallites was slow. It is likely that the increased concentration of metal is sufficient to block the pores at the surface of the crystallites. The sodium concentrations quoted are nominal, and are probably larger than the true values since a fraction of the metal inevitably reacted with the silica to give the reaction vessel a brown color.

The ESR spectrum of the pink dilute sample in Fig. 2a shows a 13-line signal similar to that previously reported by Rabo *et al.* (*5*). We attribute this signal to an *ionic cluster species* Na_4^{3+} consisting of an unpaired electron interacting with four equivalent sodium nuclei (^{23}Na, $I = \frac{3}{2}$, 100% abundance). The ESR measurements are unable to determine whether one or three electrons are trapped at the cluster so the ionic cluster species should strictly be written Na_4^{N+} ($N = 1, 3$). However, we will continue to use the notation Na_4^{3+} for brevity. The ESR spectrum of the black concentrated sample in Fig. 2c shows a single-line resonance similar to that previously reported from small particles of sodium metal (*10, 11*). We attribute this signal to a *metallic cluster species* consisting of metallic particles within the zeolite cavities. Evidence for these assignments, and the ESR parameters of both the ionic and metallic cluster species are given below.

The ESR spectrum of the dark-red intermediate sample in Fig. 2b shows signals from both the ionic clusters and the metallic clusters. Experiments shows that the relative proportions of the two signals varies monotonically with the concentration of sodium; the ionic cluster signal decreases in strength relative to the metallic cluster signal as the nominal metal concentration increases. There is also a marked difference in the microwave power saturation behavior of the two species as shown in Fig. 3;

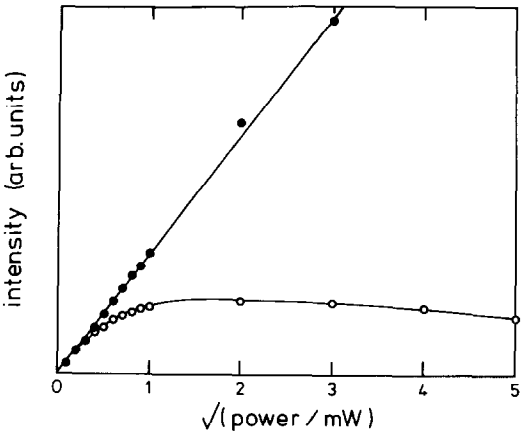

FIG. 3. Signal amplitude in arbitrary units as a function of microwave power for the ionic cluster signal (open circles) and the metallic cluster signal (filled circles) in samples of zeolite Na-Y reacted with sodium vapor.

the amplitude of the ionic cluster signal saturates if the power is greater than ~2 mW, whereas the amplitude of the metallic cluster signal did not saturate even if the power was increased above 200 mW. It is therefore possible to suppress a strong ionic cluster signal and reveal a weak underlying metallic cluster signal. The shape of the saturation curve of the ionic cluster signal suggests that the hyperfine lines are inhomogeneously broadened (*12*), and this is probably caused by superhyperfine interactions with the nuclei of the silicon or aluminum framework atoms. ENDOR measurements are under way to clarify this. The saturation properties of the metallic cluster signal suggests that this signal is homogeneously broadened.

The ESR parameters of the ionic cluster signal in Fig. 2a are essentially identical to those determined by Rabo *et al.* (*5*). The isotropic g-value of the signal is measured to be 1.999 ± 0.001 and there is a uniform separation of 32.1 ± 0.1 G between the 13 hyperfine lines. The overall separation between the outermost hyperfine lines is then 385.2 G. The first-derivative peak-to-peak

linewidth of each of the hyperfine lines is of the order of 10 G. None of these parameters change noticeably with temperature; the spectrum at 10 K is identical to the spectrum at 300 K. However, the intensity of the signal decreases with increasing temperature suggesting a Curie-type paramagnetic susceptibility although we have not yet made quantitative intensity measurements. The ionic cluster signal does not change noticeably with increasing metal concentration; both the g-value and the separation between the hyperfine lines remain constant within the above limits.

The metallic cluster signal in Fig. 2c has an isotropic g-value of 1.9997 ± 0.0005, and a linewidth of 8 G at 120 K. The g-value did not vary with temperature over the range 120–300 K within the quoted limits, but the linewidth increased slightly to 9 G at room temperature. The intensity of the signal decreases with increasing temperature again suggesting a Curie-type paramagnetic susceptibility rather than the Pauli-type paramagnetic susceptibility of a bulk metal. The signal has an approximately Lorentzian shape, although there is more intensity in the wings of the spectrum than expected. This is probably due to a distribution of particle sizes (*10*) since there is a significant decrease in the linewidth with increasing metal concentration at any particular temperature. When the metallic cluster signal first appears superimposed with the ionic cluster signal, the room-temperature linewidth of the underlying metallic cluster signal is of the order of 40 G. When the underlying ionic cluster signal finally disappears at high metal concentrations, the room-temperature linewidth of the metallic cluster signal has narrowed to 9 G.

The concentrated samples did not significantly reduce the Q-factor of the microwave cavity, suggesting that the electrical conductivity of the samples is not very high. In fact at extremely high sodium concentrations, the metallic cluster signal is observed to change from the symmetric, Lorentzian shape to an asymmetric, Dyson shape characteristic of conduction-electron spin resonance (CESR) in metallic samples. This changeover is anticipated to occur when the microwave skin depth (~8000 Å in bulk sodium metal at 120 K) becomes smaller than the metallic particle dimensions. Under these circumstances, it is likely that the metal has now coated the surface of the crystallites.

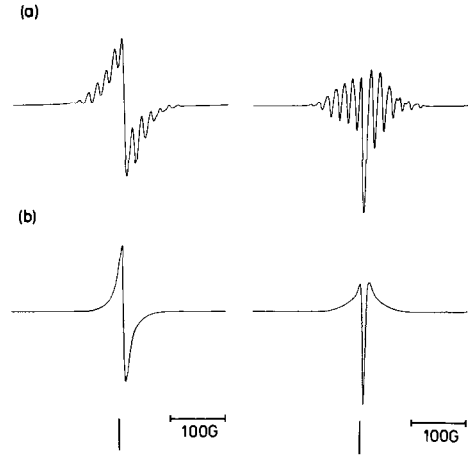

FIG. 4. First-derivative and second-derivative ESR spectra (120 K) of samples of zeolite K-Y reacted with potassium vapor. The marker corresponds to a DPPH signal at $g = 2.0036$.

Zeolite Y Containing Potassium Cations

The ESR spectra obtained at 120 K from two samples of zeolite K-Y reacted with potassium vapor are shown in Fig. 4. The metal concentrations of the two samples are similar to those of the intermediate and concentrated sodium zeolite Na-Y samples in Fig. 2, and the spectra show strong similarities to their intermediate and concentrated sodium counterparts. The potassium samples are dark-blue and black, respectively. In particular, both a 13-line ionic cluster signal and a single-line metallic cluster signal are observed. The ionic clusters appear to be unstable, however, and pro-

longed heating causes the ionic clusters to transform to small metallic particles. For this reason, samples were usually removed from the tube furnace before all of the potassium metal had reacted with the zeolite in an attempt to "quench in" the ionic clusters. In the discussion below, we concentrate upon the differences in the ESR parameters of the corresponding sodium and potassium species.

We attribute the 13-line signal to an ionic cluster species K_4^{3+} consisting of an unpaired electron interacting with four equivalent potassium nuclei (^{39}K, $I = \frac{3}{2}$, 93.1% abundance; ^{41}K, $I = \frac{3}{2}$, 6.9% abundance). The g-value of the ionic cluster signal in Fig. 4a is measured to be 1.996 ± 0.001 and there is a uniform separation of 16.4 ± 0.1 G between the *principal* set of 13 hyperfine lines. The overall separation between the outermost hyperfine lines is then 196.8 G. The linewidth of each of the hyperfine lines is of the order of 5 G. In addition, further hyperfine structure is visible in the wings of the spectrum particularly on the high-field side; this structure is particularly prominent in the second-derivative spectrum. Since potassium has two stable isotopes, we have to consider the possible permutations of these isotopes among the four potassium nuclei comprising the ionic cluster.

Approximately 75% of the clusters contain four ^{39}K cations, and these clusters should give rise to the principal set of hyperfine lines. The majority of the remaining clusters will contain three ^{39}K cations and one ^{41}K cation; and these clusters should give rise to additional hyerfine lines. The magnetic moment of the ^{41}K nucleus is approximately half that of the ^{39}K nucleus, and so these hyperfine lines should be closer to the center of the spectrum as observed. This hypothesis does not explain, however, why the additional hyperfine lines are more prominent on the high-field side of the spectrum. It is possible that the cluster of four potassium cations is slightly distorted, giving rise to anisotropy in the g-values and hyperfine splittings. Spectral simulation studies and further measurements at a higher microwave frequency are underway to clarify this effect.

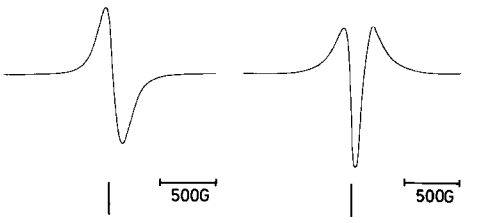

FIG. 5. First-derivative and second-derivative ESR spectra (120 K) of a sample of zeolite Rb-Y reacted with rubidium vapor. The marker corresponds to a DPPH signal at $g = 2.0036$.

The metallic cluster signal in Fig. 4b has an isotropic g-value of 1.9978 ± 0.0005, and a linewidth of 8 G at 120 K. Neither the g-value or the linewidth vary with temperature over the range 120–300 K within the quoted limits.

Zeolite Y Containing Rubidium Cations

The ESR spectra obtained at 120 K from a sample of zeolite Rb-Y reacted with rubidium vapor are shown in Fig. 5. The metal concentration of this black sample is similar to that of the concentrated zeolite Na-Y sample in Fig. 2, and a single-line, metallic cluster signal is observed. We have so far been unable to detect a Rb_4^{3+} ionic cluster species (^{85}Rb, $I = \frac{5}{2}$, 72.8% abundance; ^{87}Rb, $I = \frac{3}{2}$, 27.2% abundance) in any of the zeolite Rb-Y samples examined. In view of the properties of the two rubidium isotopes, the signal of these ionic clusters would exhibit many hyperfine lines and may be difficult to detect. However, we believe that the rubidium ionic clusters either do not form at all, or are unstable with respect to small metallic particles. In addition to the metallic cluster signal, a weak signal from Na_4^{3+} ionic clusters was detected at low microwave powers. It is likely that a few of the

sodium cations in the parent zeolite Y have not been exchanged by rubidium cations (*9*).

The metallic cluster signal in Fig. 5 has an isotropic g-value of 1.989 ± 0.001, and a linewidth of 145 G at 120 K. The g-value did not vary with temperature over the range 120–300 K within the quoted limits, but the linewidth decreased considerably to 115 G at room temperature.

Mixed-Metal Samples

Having discussed the results obtained from samples formed by reacting a zeolite Y containing alkali-metal cations with the *same* alkali-metal vapor, we now turn to the results obtained by reacting the zeolite Y with the vapor of an alkali-metal *different* from the cations. No further ionic cluster species have been detected, however, and our results suggest that the nature of the ionic cluster is determined *only* by the nature of alkali-metal cations in the zeolite before the reaction with the alkali-metal vapor. For example, the reaction of zeolite Na-Y with potassium vapor results in the formation of Na_4^{3+} clusters. Conversely, the reaction of zeolite K-Y with sodium vapor results in the formation of K_4^{3+} clusters.

Discussion

Ionic Clusters

Exposure to a low concentration of alkali-metal vapor results in brightly colored samples with an ESR signal characteristic of an ionic cluster species M_4^{3+}. An unpaired electron is trapped at a cluster of four equivalent alkali-metal cations M^+ which are presumably located at the vertices of a tetrahedron. The stability of the ionic clusters appears to decrease as the atomic number of the alkali metal increases: the Na_4^{3+} clusters were quite stable, the K_4^{3+} clusters less stable, and Rb_4^{3+} clusters, if they form, unstable with respect to small metallic particles. In this section, we consider the location of these clusters within the zeolite cavities and the variation in their stability.

Rabo *et al.* (*5*) suggested that the formation of the Na_4^{3+} clusters in zeolite Na-Y reacted with sodium vapor occurs via the reaction

$$3Na^+ + Na^0 \rightarrow Na_4^{3+} \qquad (1)$$

A guest sodium atom diffuses into the zeolite to be ionized by the strong electrostatic fields inside the cavities. The unpaired-electron wavefunction then encompasses the four sodium cations to form the observed ionic cluster. However, the formation of the same ionic clusters in zeolite Na-Y reacted with potassium or rubidium vapor demonstrates that the four sodium cations forming the ionic cluster are resident in the zeolite before the reaction. Thus the potassium or rubidium cations formed by ionization of the guest potassium or rubidium atoms do not form part of the ionic cluster, and the reaction (1) may be generalized to the reaction

$$4Na^+ + M^0 \rightarrow Na_4^{3+} + M^+ \qquad (2)$$

The guest metal atoms M are able to reduce the metal cations in the zeolite to form the ionic clusters. The eventual location of the resulting guest metal cations M^+ is unknown.

Other ionic cluster species have been formed by the reduction of metal cations in zeolites. ESR spectra recorded *during* the reduction of zeolite Ag-A by hydrogen gas showed ESR signals characteristic of an ionic cluster species Ag_6^{N+} ($N = 1, 3, 5$) in which an unpaired electron is trapped at a cluster of six equivalent silver cations presumably located at the vertices of an octahedron (*13*). It was argued that these ionic clusters were located in the sodalite cages. As the reduction proceeded, the intensity of the ionic cluster signal decreased while a signal from small particles of silver grew in

intensity until only the signal from the metal particles was visible. Further reduction caused the partial breakdown of the aluminosilicate lattice, increasing the metallic particle size and hence decreasing the linewidth of the metallic particle signal (see below). Finally, very large metallic particles were formed on the surface of the crystallites. It is possible that a similar sequence of events occurs in the reduction of zeolite Rb-Y by rubidium vapor.

We propose that the alkali-metal ionic clusters are also located in the sodalite cages of the zeolite Y. To test this hypothesis, we have investigated the formation of ionic clusters in zeolite A which has smaller α-cages than zeolite Y. The identical ionic cluster species with a hyperfine splitting of 32 G was indeed formed in samples of zeolite Na-A reacted with sodium vapor but only with difficulty; the coloration of the zeolite required longer reaction times. Despite considerable effort, we have been unable to produce the ionic cluster species Na_4^{3+} in isolation; the most dilute colored samples were lilac and comprised a mixture of the pink ionic cluster species with the dark-colored metallic cluster species. Both the reduced accessibility of the sodalite cages, and the increased number of sodium cations may hinder the formation of the ionic clusters. The longer reaction times may then transform the ionic clusters into small metallic particles. Very similar results were obtained when samples of Na-sodalite containing only sodalite cages were reacted with sodium vapor (*14*); the dilute samples also comprised a mixture of the ionic cluster species with a hyperfine splitting of 32 G and the metallic cluster species. In summary, the fact that identical Na_4^{3+} ionic cluster species are observed in zeolite Y, zeolite A, and in sodalite strongly suggests that the ionic clusters are located in the sodalite cages in all three materials. The results obtained with the mixed metal samples show that the reduction of the alkali-metal cations within the sodalite cages is likely to occur by electron transfer through the 2.2-Å pores into the sodalite cages.

Having postulated that the ionic clusters occur in the sodalite cages, it is of interest to compare the dimensions of these tetrahedral clusters with the 6.5-Å diameter of the sodalite cages. Since the unpaired electron resides equally on the four alkali-metal cations, it is anticipated that the distance between the nuclei is small and comparable to the internuclear distance in the bulk metal (*15*). With the assumption of the bulk metal internuclear distance, we can derive "metallic" radii and calculate the approximate dimensions of the tetrahedral clusters: sodium 8.3 Å, potassium 10.0 Å, and rubidium 11.0 Å.

The clusters are calculated to be larger than the sodalite cages, but the "metallic" radii are almost certainly too large to represent accurately the cations comprising the cluster. Conversely, the corresponding ionic radii (*15*) are probably too small. It is likely that an intermediate value is more appropriate, and that the stability of the cluster species can be related to their size: the Na_4^{3+} clusters are stable because they fit easily into the sodalite cages, the K_4^{3+} clusters are less stable and slightly distorted due to the tight fit, and the Rb_4^{3+} clusters are too large to fit inside the sodalite cages.

From the separation of the hyperfine lines in the spectrum we can deduce the percentage "atomic character" of the unpaired-electron wavefunction. A low atomic character would suggest a low occupation of the metal cation *n*s orbitals and that the unpaired-electron wavefunction is comparatively diffuse. Conversely, a high atomic character would suggest a greater occupation of the metal cation *n*s orbitals and a greater confinement of the unpaired-electron wavefunction within the ionic cluster. This confinement might reduce the stability of the ionic clusters. The unpaired electron residues equally on the four alkali-

metal cations giving rise to 13 hyperfine lines separated by Δ. The electron therefore spends 25% of the time on any particular alkali-metal cation; if the electron spent 100% of the time on an alkali-metal cation it would give rise to four hyperfine lines separated by 4 × Δ. In the spectrum of an isolated gaseous ^{23}Na atom, the four hyperfine lines are separated by 316.1 G (*16*) and so the percentage atomic character of this ionic cluster is (4 × 32.1)/316.1 = 41%. Similarly, in the spectrum of an isolated gaseous ^{39}K atom, the four hyperfine lines are separated by 82.4 G (*16*) and so the percentage atomic character of this ionic cluster is (4 × 16.4)/82.4 = 80%. The increased atomic character of the potassium cluster therefore supports the hypothesis that the potassium cluster is more compressed and possibly less stable than the sodium cluster. The corresponding rubidium clusters would be even less stable.

Metallic Clusters

Exposure to a high concentration of alkali-metal vapor results in dark-colored samples with an ESR signal characteristic of small metallic particles. In this section, we consider the possible relaxation mechanisms of the conduction-electron spins within these metallic particles, and discuss the variation of the *g*-value and linewidth of the signal for sodium, potassium, and rubidium particles as the particle size varies. The *g*-values of the ionic and metallic cluster signals observed in samples of zeolites Na-Y, K-Y, and Rb-Y exposed to the corresponding alkali-metal vapor are shown in Table I. Also shown for comparison are the *g*-values of the much larger metal particles (~1000 Å and above) obtained in frozen solutions of the alkali metals in a nonaqueous solvent (*17, 18*), and the corresponding *g*-values of the bulk metals (*19, 20*). It is convenient to define a *g*-shift, Δg, as the deviation of the *g*-value from the free-spin value of 2.0023; viz. $\Delta g = g_{obs} - 2.0023$.

TABLE I

THE *g*-VALUES FOR VARIOUS ALKALI-METAL SPECIES

Species	Metal		
	Sodium	Potassium	Rubidium
Ionic clusters	1.999 (−0.003)	1.995 (−0.008)	—
Metallic clusters	1.9997 (−0.0026)	1.9978 (−0.0045)	1.989 (−0.013)
Metallic particles[a]	2.0013 (−0.0010)	1.9984 (−0.0039)	1.9917 (−0.0106)
Bulk metal[b]	2.0015 (−0.0008)	1.9997 (−0.0026)	1.9984 (−0.0039)

Note. The values in brackets are the deviation Δg of the *g*-values from the free-spin value of 2.0023; viz. $\Delta g = g_{obs} - 2.0023$.

[a] In frozen HMPA solutions; data taken from Refs. (*17, 18*).

[b] Data taken from Refs. (*19, 20*).

The spin-relaxation mechanisms of the conduction electrons in alkali-metal particles were first considered by Elliott (*21*). The electrical resistivity of the metal is principally determined by the rate of collision of the electrons with (1) the lattice vibrations; (2) the surface of the particles; and (3) the impurities in the particles. The rate of collisions due to (1) varies with temperature but is approximately independent of the particle size. Conversely, the rate of collisions due to (2) varies with particle size but is approximately independent of temperature. Finally, the rate of collisions due to (3) is approximately independent of both the temperature and particle size.

These collisions cause electronic transitions to occur within the quasicontinuous distribution of energy states in the particles; a fraction of these transitions also reverse the orientation of the electron spins resulting in spin relaxation. Thus the spin-relaxation rate of the conduction electrons is approximately proportional to the electrical resistivity of the metal. The fraction of the transitions which reverse the orientation of the electron spins varies as the square of the spin–orbit interaction of the metal, and the *g*-shift of the ESR signal var-

ies directly with the magnitude of the spin–orbit interaction. Since the spin–orbit interaction increases rapidly with increasing atomic number (*22*), low temperatures are normally required to observe an ESR signal in the heavier alkali metals. The observation of a metallic cluster species at room temperature in zeolite Rb-Y is therefore remarkable, and indicates an inhibition of the bulk metal spin-relaxation mechanisms.

The spin-relaxation rate in metal particles depends critically upon their size. If the particles are sufficiently large for the separation of the energy states to be small compared with the Zeeman energy, the surface scattering rate, and hence the linewidth of the ESR signal vary inversely with the diameter of the particles. Phonon scattering causes the linewidth to increase with increasing temperature in a similar fashion to that of the bulk metal (*10*). In addition, the paramagnetic susceptibility of the particles follows a Pauli-type variation with temperature. Conversely, if the particles are sufficiently small for the separation of the energy states to be large compared with the Zeeman energy (*23*), both the surface-scattering and phonon-scattering mechanisms are quenched. Kawabata (*24*) predicted that the linewidth of the ESR signal would then vary as the square of the particle diameter. Consequently, narrow ESR signals could be observed at comparatively high temperatures even in the heavier alkali metals. In addition, the paramagnetic susceptibility of the particles would follow a Curie-type variation with temperature.

This so-called "quantum-size" effect was predicted to occur in sodium particles smaller than ~100 Å (*24*), which is much larger than the particles postulated in the zeolite cavities. To investigate this effect, Gordon (*10*) and Smithard (*11*) studied the ESR spectra of the small sodium particles (~10 to ~1000 Å) formed by irradiation and subsequent annealing of sodium azide samples. The size of the sodium particles increased monotonically with the annealing time of the samples, allowing the ESR signals of the sodium particles to be studied as a function of their size. Narrow ESR signals arising from the quantum-size effect were not observed, however, and the linewidth of the ESR signal decreased smoothly as the size of the particles increased. Gordon (*10*) did observe an additional broad ESR signal which saturated at a low microwave power, and he suggested that the signal represented an envelope of hyperfine lines from particles small enough to exhibit the quantum-size effect. A distribution of particle sizes prevented the resolution of the individual hyperfine lines. This ESR signal is somewhat reminiscent of the ionic cluster signal observed in the zeolite cavities.

With these points in mind, we now consider the *g*-shifts and linewidths of the ESR signals of the metallic cluster species in Table I. As expected, the *g*-shifts of all the species increase as the atomic number and hence the spin–orbit interaction of the alkali metal increases. The *g*-shifts for any particular alkali metal also appear to increase as the size of the metal particles is reduced; viz. from the bulk metal to the large metallic particles in the frozen nonaqueous solvent through to the metallic clusters in zeolite Y. This increase is comparatively small, however, and the *g*-shifts do not vary appreciably with particle size or temperature.

The linewidth of the ESR signal of the metallic clusters in zeolite Y narrows significantly with increasing particle size due to the decreasing surface relaxation rate. However, the temperature dependence of the linewidth is unusual. In the concentrated sample of zeolite Na-Y, the linewidth increases by several Gauss as the temperature is increased in agreement with the signal in the bulk metal (*19*). In the concentrated sample of zeolite K-Y, the linewidth remains independent of temperature. Fi-

nally, in the sample of zeolite Rb-Y, the linewidth decreases significantly with increasing temperature in complete contrast to the signal in the bulk metal (*20*). A possible explanation relies on the relative size of the atoms: more sodium atoms can fit into the zeolite cavities than can rubidium atoms. Thus the sodium metallic clusters are possibly larger than the rubidium metallic clusters and hence have properties more similar to those of the bulk metal. Further work is needed to resolve this question.

In summary, the metallic cluster signals observed in the concentrated samples are characteristic of small particles of alkali metal located within the zeolite cavities. The particles of the heavier alkali metals, in particular, are small enough to quench the usual rapid spin-relaxation mechanisms. These metal-loaded zeolites may therefore be ideal materials to study the unusual electronic properties of small metallic particles.

Acknowledgments

The research at Cambridge was supported by the SERC (UK) and the BP Research Centre, Sunbury, England. The research at Cornell was supported by the National Science Foundation (USA) and the Materials Science Centre at Cornell University. The Cambridge/Cornell collaboration was made possible by a NATO award (Grant 250.81) to PPE and the late Professor M. J. Sienko.

References

1. R. M. BARRER, "Zeolites and Clay Minerals as Sorbents and Molecular Sieves," Academic Press, New York/London (1982).
2. D. W. BRECK, "Zeolite Molecular Sieves: Structure, Chemistry and Use," Wiley, London (1974).
3. C. A. FYFE, J. M. THOMAS, J. KLINOWSKI, AND G. C. GOBBI, *Angew. Chem. Int. Ed. Engl.* **22,** 259 (1983).
4. P. H. KASAI, *J. Chem. Phys.* **43,** 3322 (1965).
5. J. A. RABO, C. L. ANGELL, P. H. KASAI, AND V. SCHOMAKER, *Discuss. Faraday Soc.* **41,** 328 (1966).
6. J. A. RABO AND P. H. KASAI, *Progr. Solid State Chem.* **9,** 1 (1975).
7. J. M. THOMAS, *Ultramicroscopy* **8,** 13 (1982).
8. J. M. THOMAS, S. RAMDAS, G. R. MILLWARD, J. KLINOWSKI, M. AUDIER, J. GONZALES-CALBERT, AND C. A. FYFE, *J. Solid State Chem.* **45,** 368 (1982).
9. H. S. SHERRY, *J. Phys. Chem.* **70,** 1158 (1966).
10. D. A. GORDON, *Phys. Rev. B* **13,** 3738 (1976).
11. M. A. SMITHARD, *Solid State Commun.* **14,** 411 (1974).
12. C. P. POOLE, "Electron Spin Resonance," Wiley, London (1983).
13. D. HERMESCHMIDT AND R. HAUL, *Ber. Bunsenges. Phys. Chem.* **84,** 902 (1980).
14. R. M. BARRER AND J. F. COLE, *J. Phys. Chem. Solids* **29,** 1755 (1968).
15. "CRC Handbook of Chemistry and Physics," CRC Press, Boca Raton, Florida (1983).
16. R. CATTERALL AND P. P. EDWARDS, *Adv. Molec. Relax. Processes* **13,** 123 (1978).
17. R. CATTERALL AND P. P. EDWARDS, *Adv. Molec. Relax. Processes* **7,** 87 (1975).
18. S. C. GUY AND P. P. EDWARDS, *Chem. Phys. Lett.* **86,** 150 (1982).
19. F. BEUNEU AND P. MONOD, *Phys. Rev. B* **18,** 2422 (1978).
20. W. M. WALSH, L. W. RUPP, AND P. H. SCHMIDT, *Phys. Rev. Lett.* **16,** 181 (1981).
21. R. J. ELLIOTT, *Phys. Rev.* **96,** 266 (1954).
22. Y. YAFET, *Solid State Phys.* **14,** 1 (1963).
23. R. KUBO, *J. Phys. Soc. Jpn.* **17,** 975 (1962).
24. A. KAWABATA, *J. Phys. Soc. Jpn.* **29,** 902 (1970).